HHS Public Access

Author manuscript

Clin Cancer Res. Author manuscript; available in PMC 2024 February 15.

Published in final edited form as:

Clin Cancer Res. 2023 August 15; 29(16): 3237–3249. doi:10.1158/1078-0432.CCR-23-0375.

Targeting BCL2 overcomes resistance and augments response to aurora kinase B inhibition by AZD2811 in small cell lung cancer

Kavya Ramkumar[1,*], **Azusa Tanimoto**[1,*], **Carminia M. Della Corte**[2], **C. Allison Stewart**[1], **Qi Wang**[3], **Li Shen**[3], **Robert J. Cardnell**[1], **Jing Wang**[3], **Urszula M. Polanska**[4], **Courtney Andersen**[5], **Jamal Saeh**[5], **J. Elizabeth Pease**[4], **Jon Travers**[4], **Giulia Fabbri**[6], **Carl M. Gay**[1], **Jelena Urosevic**[4,*], **Lauren A. Byers**[1,#]

[1] Department of Thoracic/Head & Neck Medical Oncology, the University of Texas MD Anderson Cancer Center, Houston, TX 77030, USA

[2] Department of Precision Medicine, University of Campania Luigi Vanvitelli, Naples, Italy

[3] Department of Bioinformatics and Computational Biology, the University of Texas MD Anderson Cancer Center, Houston, TX 77030, USA

[4] Bioscience, Research and Early Development, Oncology R&D, AstraZeneca, Cambridge, UK

[5] Bioscience, Research and Early Development, Oncology R&D, AstraZeneca, Waltham, USA

[6] Translational Medicine, Research and Early Development, Oncology R&D, AstraZeneca, Waltham, USA

Abstract

Purpose: Therapeutic resistance to frontline therapy develops rapidly in small cell lung cancer (SCLC). Treatment options are also limited by the lack of targetable driver mutations. Therefore, there is an unmet need for developing better therapeutic strategies and biomarkers of response. AURKB inhibition exploits an inherent genomic vulnerability in SCLC and is a promising therapeutic approach. Here, we identify biomarkers of response and develop rational combinations with AURKB inhibition to improve treatment efficacy.

Experimental design: Selective AURKB inhibitor AZD2811 was profiled in a large panel of SCLC cell lines (n=57) and patient-derived xenograft (PDX) models. Proteomic and transcriptomic profiles were analyzed to identify candidate biomarkers of response and resistance.

[#] **Corresponding author:** Lauren A. Byers, 1515 Holcombe Blvd., Unit 432, Houston, Texas, 77030. Phone: (713) 745-2982; Fax: (713) 792-1220; lbyers@mdanderson.org.

[*]These authors contributed equally

Conflict of interest statement

L.A.B. receives research support from AstraZeneca and Amgen, and serves in consulting/advisory roles for Merck Sharp & Dohme Corp., Arrowhead Pharmaceuticals, Chugai Pharma, AstraZeneca, Genetech Inc., Abbvie, BeiGene, Jazz Pharmaceuticals. C.M.G. serves on advisory boards for AstraZeneca, Bristol-Myers Squibb, Jazz Pharmaceuticals and MonteRosa, and on the speaker's bureau for AstraZeneca, BeiGene and Jazz Pharmaceuticals. C.M.G has also received research support from AstraZeneca. C.M.D. has received travel grants from Amgen and AstraZeneca, and personal speaker fee from Roche, MSD and Merck. U.P, C.A., J.S., J.E.P. J.T., G.F. and J.U. were employees of AstraZeneca and shareholders when the data for this manuscript was generated. All other authors declare no competing interests.

Effects on polyploidy, DNA damage and apoptosis were measured by flow cytometry and western blotting. Rational drug combinations were validated in SCLC cell lines and PDX models.

Results: AZD2811 showed potent growth inhibitory activity in a subset of SCLC, often characterized by, but not limited to, high cMYC expression. Importantly, high BCL2 expression predicted resistance to AURKB inhibitor response in SCLC, independent of cMYC status. AZD2811-induced DNA damage and apoptosis were suppressed by high BCL2 levels, while combining AZD2811 with a BCL2 inhibitor significantly sensitized resistant models. *In vivo*, sustained tumor growth reduction and regression was achieved even with intermittent dosing of AZD2811 and venetoclax, an FDA approved BCL2 inhibitor.

Conclusions: BCL2 inhibition overcomes intrinsic resistance and enhances sensitivity to AURKB inhibition in SCLC preclinical models.

Keywords

Aurora kinase B inhibition; AURKB; AZD2811; BCL2; Venetoclax; SCLC; Resistance; cMYC

Introduction

Small cell lung cancer (SCLC) is an aggressive lung tumor of neuroendocrine origin with poor prognosis[1] and limited treatment options[2]. Therapeutic resistance to the standard of care treatment (a combination of chemotherapy and immunotherapy) also emerges rapidly, necessitating the need for new and effective treatment approaches, particularly in the relapsed setting[2]. SCLC is characterized by a near universal loss of *TP53* and *RB1* tumor suppressor genes [3]. About 20% of SCLC tumors also exhibit genomic amplification of the *MYC* oncogene[3–5]. While the paucity of targetable oncogenic driver mutations in SCLC has precluded the development of effective targeted therapies, the genomic and proteomic alterations prevalent in SCLC have been shown to induce targetable synthetic lethal dependencies[6]. AURKs are key regulators of mitosis entry and progression. Aurora kinase A (AURKA) regulates mitotic entry, spindle assembly and centrosome function[7]. Aurora kinase B (AURKB), however, forms an integral part of the chromosome passenger complex and regulates chromosome condensation, kinetochore attachment and spindle assembly checkpoint, ensuring proper chromosomal segregation and cytokinesis[8,9]. Both AURKs are upregulated by MYC and have been shown to be essential for the maintenance of MYC-driven cancers[10,11]. Given their roles in tumorigenesis and overexpression in many cancers, AURK inhibitors have been investigated as potential therapeutic agents[12–14]. Small molecule inhibitors of AURKA and AURKB, such as alisertib and barasertib, have shown promising activity in preclinical SCLC models, particularly in those with high MYC and NEUROD1 expression[15–18]. Retrospective analyses have also shown that relapsed SCLC patients, particularly those with high cMYC expression, had a relatively better treatment outcome with alisertib/paclitaxel compared to placebo, underscoring the need for testing AURK inhibitors in biomarker-defined patient cohorts[19].

In this study, we evaluated the therapeutic potential of AURKB inhibition by a selective inhibitor, AZD2811 (also known as AZD1152 hydroxyquinazoline pyrazol anilide; AZD1152-hQPA)[20], using *in vitro* and *in vivo* models that recapitulate the genomic and

proteomic heterogeneity in SCLC. AZD2811 has also been recently evaluated in Phase I clinical trial in SCLC (NCT02579226, NCT04745689)[21]. We report here biomarkers of response and rational combinations to address resistance to single agent AZD2811. Overall, the findings of this study provide promising preclinical proof-of-concept that the rational and biomarker-driven combinations of AZD2811 could be an effective treatment strategy in SCLC.

Materials and Methods

Reagents.

Antibodies for western blotting purchased from Cell signaling: BCL2 (#15071, 1:1000, RRID:AB_2744528), BCL-xL (#2764, 1:1000, RRID:AB_2228008), cleaved PARP (#5625, 1:1000, RRID:AB_10699459), γH2AX (#9718, 1:1000, RRID:AB_2118009), phospho-Histone H3 (S10) (#53348, 1:1000, RRID:AB_2799431) and Santa Cruz Biotechnology: β-actin (sc-47778, 1:2000, RRID:AB_626632). AZD2811 was provided by AstraZeneca. Venetoclax was purchased from Selleck Chemicals. Propidium iodide was purchased from Sigma-Aldrich. RNase A (EN0531) and FITC Annexin V apoptosis detection kit (#556547) were purchased from Thermo scientific and BD Pharmingen, respectively.

Cell lines.

Human SCLC cell lines were purchased from ATCC or Sigma-Aldrich. The human patient-derived xenograft (PDX) cell line NJH29 was generously provided by Dr. Julien Sage (Stanford University, Stanford, CA, USA). Cell lines were cultured in RPMI, supplemented with 10% fetal bovine serum and 100 IU/mL penicillin and 100 μg/mL streptomycin, unless otherwise specified by ATCC, at 372E°C in a humidified chamber with 5% CO_2. All cell lines were authenticated by STR profiling, maintained in culture for less than two months and tested regularly for *Mycoplasma* contamination using MycoAlert Plus (Lonza).

Generation of isogenic BCL2-overexpressing cell lines.

SCLC cells (2×10^5) were transfected with either pLOC lentiviral vectors expressing wild-type human BCL2 or empty plasmid using polybrene (4μg/ml). The lentivirus-containing medium was removed 12 h later following transfection. The cells infected with the lentivirus vectors were continuously selected using blasticidin (Wako). BCL2 overexpression was confirmed by western blotting.

siRNA knockdown.

SCLC cells (2×10^5), cultured in the medium containing 10% FBS for 24 h, were transfected with Silencer®Select BCL2 siRNA (#4392420), BCL-xL siRNA (#4390824) or negative control #1 siRNA (#4390843) (Thermo Scientific) using Lipofectamine RNAiMAX for 48 h.

Cell viability assays.

SCLC cell lines and BCL2-overexpressing isogenic cell lines were seeded at a density of 2000 cells/well in 96-well white bottom microtiter plates and treated with DMSO control or

AZD2811 at different concentrations in triplicate for 96 h. Cell viability was measured using CellTiter-Glo (Promega) and luminescence was read on a Synergy HT microplate reader (BioTek). For single drug treatments, dose response curves were modeled by non-linear curve fitting and the IC_{50} values were estimated using our previously published drexplorer software[45]. Replicate reproducibility was determined by concordance correlation coefficient and goodness of fit by residual standard error. For drug combination experiments, cells were treated with AZD2811 and/or venetoclax (or BCL-xL inhibitor) or with DMSO control. The area under the curve (AUC) for the observed effect of the combination was compared to the AUC for the additive effect predicted by the BLISS model. The difference between the two AUCs, denoted by ΔAUC, was computed. ΔAUC values < -0.1 was considered to be a greater than additive; based on an estimated 10% margin of experimental variability[45].

Reverse phase protein array (RPPA).

Proteomic expression of SCLC cell lines was performed as described previously[23].

Western blotting.

Cells (1×10^6) were seeded in 10 cm dishes and treated as indicated for 48 h. Cells were collected by centrifugation at 1,500 rpm for 5 min and washed with ice-cold PBS. The cell pellet was then lysed with RPPA lysis buffer supplemented with protease and phosphatase inhibitor cocktail. The lysate was centrifuged at 14,000 rpm for 10 min to remove cell debris. Total protein concentration of the supernatant was measured using DC protein assay reagent (Biorad). 30 μg of cell lysate was boiled for 5 min at 95°C with 4X laemmli buffer, resolved on a 10 or 15% polyacrylamide gel and electroblotted onto a nitrocellulose membrane. Membranes were blocked in 1X Caesin blocking solution (Biorad) for 1 hour at room temperature and incubated overnight with primary antibodies at specified dilutions at 4°C. The membranes were then washed with Tris-buffered saline with 0.1% Tween-20 (TBST) and incubated with appropriate horseradish peroxidase-linked secondary antibodies (Santa Cruz Biotechnology anti-mouse (sc-516102, 1:2000, RRID:AB_2687626), Cell signaling anti-rabbit (#7074, 1:2000, RRID:AB_2099233) for 12Eh at room temperature. The immunoblots were visualized using the SuperSignal West Pico Plus chemiluminescent substrate (Thermo Scientific) on a Biorad ChemiDoc™ Touch imaging system. Tumor fragments were homogenized and subjected to western blotting similarly.

Cell cycle analysis.

0.5×10^6 cells were plated in a 60 mm dish and treated with DMSO or AZD2811 (30 nM). Cells were harvested at 48h, washed with ice-cold PBS and fixed in 70% cold ethanol overnight at 4°C. Cells were collected by centrifugation, washed twice with cold PBS and stained with 50μg/mL propidium iodide and 250μg/mL RNAase A for 1 h at 37°C. Cells were analyzed on a Gallios cell analyzer (Beckman Coulter) and data was analyzed using Flow Jo software (Treestar, San Carlos, CA) (RRID:SCR_008520).

Annexin-V apoptosis assay.

SCLC cells (0.5×10^6) were treated with indicated concentrations of AZD2811, venetoclax or their combination for 72 h and harvested. Live cells were then stained with Annexin V-FITC

antibody and propidium iodide, using the Annexin V-FITC Apoptosis Detection Kit (BD Biosciences, San Jose, CA), per the manufacturer's instructions. Cell staining was analyzed on Gallios cell analyzer (Beckman Coulter).

Caspase activity assay.

SCLC cell lines (25,000 cells/well) were treated with indicated concentrations of AZD2811, venetoclax or their combination in triplicate for 72 h in a 96-well white bottom microtiter plate. Caspase activity was measured using caspase-glo 9 assay and caspase glo 3/7 assay kits (Promega).

Animal studies.

6-week old athymic nude mice from Envigo were used for the animal experiments and maintained in strict accordance with protocols approved by the Institutional Animal Care and Use Committee of the university of Texas MD Anderson Cancer Center and the NIH Guide for the Care and Use of Laboratory Animals. All efforts were made to minimize animal suffering. Circulating tumor cells-derived xenograft (CDX) model (SC16),was generated as described previously and maintained *in vivo* by serial transplantation[26]. SC49PDX, established from the core-needle biopsy as previously described[26], was provided by Dr. Jack Roth. Low passage viable tumor fragments were implanted subcutaneously into the flank of nude mice. When tumors reached an average volume of about 100 mm^3, the mice were randomized into 2 groups and treated with vehicle or AZD2811 NP (10 mg/kg, diluted in saline, i.v. injection once a week). Tumor volumes and weights were measured every 2–3 days. Cell line xenograft experiments (H1048, H69 and H211) were done in accordance with all relevant ethical regulations for animal testing and research following AstraZeneca's global bioethics policy and received ethical approvals from the AstraZeneca ethical committee. Left flank of nude female mice were injected subcutaneously with cells resuspended in PBS. When the tumors reached nearly 200mm^3, the mice were randomized into 4 groups and treated with vehicle, AZD2811 NP (25mg/kg diluted in saline, i.v. injection once a week), venetoclax (100mg/kg, dosed orally once a day) or their combination. Mice weights were measured daily and tumor volumes were measured twice weekly.

Studies using SCLC PDX models were carried out at XenTech, France, in accordance with the French regulatory legislation concerning the protection of laboratory animals and in accordance with a currently valid license for experiments on vertebrate animals, issued by the French Ministry of Higher Education, Research and Innovation. Female athymic nude mice aged 6 to 9 weeks were anaesthetized with 100 mg/kg ketamine hydrochloride and 10mg/kg xylazine. Skin of anaesthetized mice was asepticized with a chlorhexidine solution, incised on the interscapular region, and one 20 mm^3 tumor fragment was placed in the subcutaneous tissue. Skin was closed with clips. All mice from the same experiment were implanted on the same day. Mice were randomized to the different treatment groups. For each group, 3 mice with established tumors, with tumor volume ranging 60 to 200mm^3, were included in the study. Mice were treated with AZD2811NP (25mg/kg diluted in saline, i.v. injection once a week), venetoclax (100mg/kg, dosed orally once a day), AZD0466

(34mg/kg, i.v. injection once a week) and the combination of AZD2811NP and venetoclax/ AZD0466 using above mentioned doses and schedules as indicated.

Statistical analysis.

Data statistics and bioinformatics analyses were performed using R (version 3.3.0, https://www.r-project.org/) (RRID:SCR_001905) and Bioconductor packages (https://www.bioconductor.org/). Statistical comparisons were performed using unpaired t-test for two-tailed p-value, unless specified otherwise. For RPPA expression analyses, Benjamini-Hochberg method was used to control false discovery rate (FDR)[46].

Data and material availability.

Any materials are available from the corresponding author upon reasonable request.

Results

BCL2 expression predicts resistance to the selective AURKB inhibitor AZD2811 in SCLC cell lines

A previous study showed that loss of RB1, a hallmark of SCLC, resulted in a hyper-dependency on AURKB and enhanced sensitivity to AURKB inhibition[22]. Based on this, we evaluated the effects of AZD2811, a selective AUKRB inhibitor, on cell viability in a panel of 57 SCLC cell lines, where most of them exhibited RB1 deficiency at the genetic and/or proteomic level. Interestingly, only 15/57 SCLC cell lines (26%) were highly sensitive to AZD2811 (IC_{50} < 30 nM) while 9/57 (16%) showed intermediate sensitivity (IC_{50} = 30–100nM) (Fig. 1A). A majority of SCLC cell lines (58%), despite RB1 deficiency, were highly resistant to AZD2811 (IC_{50} > 100nM, the highest concentration tested) (Fig. 1A). Our data therefore suggest that, while RB1 loss is near universal in SCLC, it is not sufficient for sensitivity to AURKB inhibition by AZD2811. Therefore, to identify potential predictors of drug response, we applied an unbiased approach by comparing the proteomic expression profiles, generated by reverse phase protein array (RPPA)[23], of SCLC cell lines that were sensitive to AZD2811 (IC_{50} < 100nM) to those that were resistant (IC_{50} > 100nM).

A synthetic lethal interaction between *MYC* overexpression and AURKB inhibition has been previously reported in other cancers[24]. *MYC*/cMYC has also been previously shown to be a biomarker of sensitivity to both AURKA and AUKRB inhibitors in SCLC[6,18,19,25]. Consistent with these, we found that the mean expression of cMYC protein was higher in AZD2811-sensitive cell lines (Fold change = 1.95, $p<0.05$) (Supplementary Fig. 1A). However, of the 24 sensitive SCLC cell lines, only 11 exhibited high cMYC levels, based on the bimodal distribution of cMYC protein expression by RPPA, while eight cell lines with high cMYC levels were resistant to AZD2811 (Fig. 1A, Supplementary table 1). Furthermore, several SCLC cell lines, even in the absence of *MYC* amplification/ cMYC overexpression, were found to be highly sensitive to AZD2811, highlighting that sensitivity to AURKB inhibition was not limited to MYC-driven SCLC.

Beyond cMYC, we found that SCLC cell lines that were resistant to AZD2811 expressed high levels of the anti-apoptotic protein BCL2 (Fold change = −1.6, p=0.06) (Fig. 1B).

No differences in the other BCL2 family members were seen. Similarly, we also found BCL2 to be inversely associated with *in vivo* AZD2811 sensitivity in patient derived xenograft models established from either the circulating tumor cells (CDX) or a core-needle biopsy (PDX) from SCLC patients, following relapse to frontline platinum therapy[26]. In two such models - MDA-SC16 (CDX) and MDA-SC49 (PDX) - where we previously reported *AURKA* and *AURKB* expression in specific cell clusters[26], we tested efficacy of the slow release nanoparticle formulation of AZD2811[27] (AZD2811NP) as a single agent at a low dose (10 mg/kg). AZD2811NP induced significant growth inhibition of the MDA-SC49 tumors, which expresses high levels of *MYC* and low levels of *BCL2*, while it had little effect on MDA-SC16 tumors, which has high *BCL2* and low *MYC* expression. (Fig. 1C).

BCL2 is frequently overexpressed in SCLC cell lines and tumors[28,29]. When we analyzed the transcriptomic profiles of 57 SCLC cell lines and 81 treatment-naïve SCLC tumors[3], *BCL2* was found to be overexpressed in both cohorts (Fig. 1D). As reported previously[17], *BCL2* mRNA expression was frequently high in many ASCL1 (SCLC-A) and POU2F3 (SCLC-P) expressing SCLC cell lines and tumors. At the proteomic level, BCL2 levels were highly correlated with BIM expression (rho=0.68, $p<0.001$) and modestly correlated with BCL-xL and phosphoBAD (rho > 0.3, $p<0.05$) (Fig. 1D). BCL2 also showed a bimodal distribution in the SCLC cell lines (bimodality index=1.73; Supplementary Fig. 1B). In line with the role cMYC plays in repressing *BCL2* expression[10], several SCLC cell lines in the BCL2-low group, which was also predominantly sensitive to AZD2811, expressed high cMYC protein levels (Fold change = 2.8, p value by t-test = 0.001) (Fig. 1E). However, overall, we observed only a modest inverse correlation between cMYC and BCL2 expression, at both mRNA (rho=−0.32, $p<0.05$) and protein levels (rho=−0.25, $p<0.05$), among the SCLC cell lines, suggesting that high cMYC expression is not always associated with low BCL2 expression. In fact, a subset of SCLC cell lines as well as tumors expressed high levels of both cMYC/*MYC* and BCL2/*BCL2* (Fig. 1D). Furthermore, these cMYC-high cell lines with high BCL2 levels were predominantly resistant to AZD2811, highlighting BCL2 as a strong predictor of resistance to AZD2811 in SCLC cell lines (p=0.011 by pearson's chi-squared test) (Fig. 1E and Supplementary Fig. 1C).

To determine if BCL2 was indeed a causal mediator of resistance to AZD2811, we generated BCL2 overexpressing isogenic cell line pairs from AZD2811-sensitive SCLC cell lines, expressing low endogenous BCL2 expression and varying cMYC levels. In 96 h cell viability assays, SCLC cell lines stably overexpressing BCL2 were consistently more resistant to AZD2811, compared to the isogenic vector-control cells, with a significant increase in IC_{50} ($p<0.004$ by paired t-test) (Fig 1F). Interestingly, a sensitive cell line (H1048), which endogenously expresses high levels of cMYC as well as BCL2, could be made more resistant to AZD2811 by further increasing BCL2 levels. Conversely, to determine if AZD2811 resistance could be reversed by reducing BCL2 expression, we transiently silenced BCL2 in AZD2811-resistant SCLC cell lines that endogenously expressed high levels of BCL2. Compared to the non-targeting control siRNA, silencing of BCL2 was sufficient to significantly enhance sensitivity to AZD2811 in these cell lines (Supplementary Fig. 1D). Thus, these results show that high BCL2 expression predicts and mediates resistance to the AURKB inhibitor, AZD2811. We also found that high BCL2

levels in SCLC cell lines were associated with resistance to the AURKA inhibitor, alisertib (Supplementary Fig. 1E,F).

AZD2811-induced polyploidy and apoptotic cell death is suppressed in BCL2-high SCLC cell lines

AURKB inhibition causes failed cytokinesis, endoreduplication and polyploidy[30,31]. Consistent with this, flow cytometry analysis showed an increase in the 8N cell population following 48 h treatment with AZD2811 (30 nM), indicating severe mitotic defects and polyploidy, in the BCL2-low sensitive cell lines. On the other hand, AZD2811 induced polyploidy in some BCL2-high resistant cell lines while it had no effect on cell cycle progression in others (Supplementary Fig. 2A). Since AURKB inhibition induced-polyploidy triggers apoptotic cell death[32,33], we next assessed apoptosis by Annexin-V and propidium iodide staining in SCLC cell lines treated with AZD2811 (30 nM) for 72 h. As expected, there was a significant increase in apoptotic cell death following AZD2811-induced polyploidy in the sensitive cell lines. In contrast, apoptosis was consistently suppressed in the AZD2811-resistant BCL2-high SCLC cell lines (Fig. 2A, Supplementary Fig. 2B).

Overexpression of BCL2 similarly mitigated induction of apoptosis by AZD2811. In the sensitive isogenic vector-control cell lines, treatment with even a low dose of AZD2811 (30 nM) strongly induced the activity of apoptosis initiator, caspase-9, albeit in a cell line-dependent manner. Apoptosis executor, caspase 3/7, activity was also similarly induced. AZD2811 treatment also significantly increased cleavage of PARP, a substrate of caspase-3 and marker of late apoptosis, in the vector-control cells (Fig. 2B, C, Supplementary Fig. 2C). Together, these data indicate activation of the apoptotic cascade following AZD2811 treatment in BCL2-low cell lines (Fig. 2B, C). In contrast, overexpression of BCL2 suppressed caspase activation and PARP cleavage in response to treatment with AZD2811 (Fig. 2B, C). Since polyploidy results in genetic instability, we examined if AZD2811 treatment also increased DNA damage. In the sensitive vector-control cell lines, treatment with AZD2811 strongly induced accumulation of γH2AX, a marker of DNA damage (Fig. 2C). In contrast, endogenous as well as AZD2811-induced DNA damage was suppressed following BCL2-overexpression. Similarly, knockdown of BCL2 restored γH2AX accumulation and PARP cleavage in response to AZD2811 treatment in the resistant BCL2-high SCLC cell lines (Fig. 2D). An increase in cleaved caspase-3 levels in response to AZD2811 treatment was also observed following BCL2 knockdown. Previous studies in other cancer types have shown that BCL-xL inactivation had a sensitizing effect on AURKB inhibitors and other anti-mitotic agents[32,34]. However, in the resistant SCLC cell lines, BCL-xL knockdown did not significantly enhance the sensitivity of the cells to AZD2811 and had no effect on the apoptotic and DNA damage responses (Supplementary Fig. 2D, 2E). Together, these results demonstrate that intrinsic resistance to AURKB inhibition in SCLC is predominantly driven by high BCL2 levels, which inhibit the induction of apoptosis and DNA damage.

Pharmacological inhibition of BCL2 sensitizes SCLC cells to AZD2811

Next, we examined whether pharmacological modulation of BCL2 could restore AZD2811 sensitivity. As shown above, BCL2-overexpressing isogenic cell lines were resistant to AZD2811. The single agent activity of a selective BCL2 inhibitor, venetoclax, in these cells was also modest. However, the addition of venetoclax markedly sensitized these BCL2-overexpressing SCLC cells to AZD2811 (ΔAUC_{BLISS} score < −0.3) (Fig. 3A, Supplementary Fig. 3A). Treatment of BCL2-overexpressing cell lines with venetoclax also restored AZD2811-induced apoptosis, indicated by increased PARP cleavage, and augmented DNA damage (γH2AX accumulation) (Fig. 3B). On the other hand, the addition of venetoclax had no effect on the sensitivity of the isogenic vector-control cell lines ($H446^{Vec}$, $H1876^{Vec}$), expressing low BCL2 levels, to AZD2811 or on apoptosis. A similar effect was also observed in inherently AZD2811-resistant SCLC cell lines. The combination of AZD2811 with venetoclax significantly reduced cell viability, as compared to either drugs as single agents (ΔAUC_{BLISS} score < −0.2) (Fig. 3C and Supplementary Fig. 3A). Interestingly, in H1048, a BCL2-high cell line that also expresses high cMYC and sensitivity to AZD2811, addition of venetoclax further improved the effect of AZD2811, highlighting that this drug combination could be effective in a BCL2-high background, irrespective of the single agent sensitivity. In comparison to BCL2 inhibition, combination with a selective BCL-xL inhibitor (A-1331852) only modestly sensitized the resistant SCLC cell lines to AZD2811 (Supplementary Fig. 3B). Treatment with the combination of AZD2811 (30nM) and venetoclax (100 nM) also significantly increased caspase 3/7 activity, cleavage of the caspase substrate PARP as well as DNA damage (Fig. 3D, E). Consistent with these observations, the fraction of cells positive for Annexin-V and propidium iodide, signaling the late apoptotic events of phosphatidylserine externalization and loss of membrane integrity, was dramatically increased at 72 h after treatment with the drug combination (Fig. 3F and Supplementary Fig. 3C). Together, these findings demonstrate that the combination of AZD2811 with a selective BCL2 inhibitor, such as venetoclax, can overcome the intrinsic resistance and enhance apoptotic response to AURKB inhibition in SCLC cell lines.

Combination of AZD2811NP with venetoclax results in sustained tumor regression in SCLC xenograft models with high BCL2 expression

We next assessed the *in vivo* efficacy of AZD2811NP in combination with venetoclax in a panel of 12 SCLC cell line-derived and patient-derived xenograft (PDX) models that are representative of the different SCLC subtypes and express different levels of BCL2 (Fig 4A). These models were treated for a duration of four weeks with AZD2811NP monotherapy, venetoclax monotherapy or their combination. As summarized in Fig. 4A, AZD2811NP induced stasis and tumor regression in seven out of 12 models, whereas venetoclax monotherapy showed tumor regression in only one *BCL2*-high model (LC-F-22). In comparison, the combination of the two drugs demonstrated greatly improved efficacy over either single agent in eight out of 12 models (Fig. 4A). In concordance with the *in vitro* data, H1048 xenograft model, with high cMYC and BCL2 expression, was sensitive to AZD2811NP *in vivo* and addition of venetoclax further improved the response (Fig. 4B). Both single agent AZD2811NP and venetoclax, and the combination thereof were well-tolerated with no significant body weight loss in mice (Supplementary Fig. 4A). Similar results were also observed in the H69 xenograft model (Fig. 4C, Supplementary Fig. 4B). In

four SCLC PDX models, with high *BCL2* expression by RNAseq, (SC101, SC96, LC-F-22 and SC61) (Fig. 4A), the combination of AZD2811NP and venetoclax showed improved anti-tumor efficacy compared to either monotherapy (Fig. 4D–G). In addition, sustained tumor growth inhibition was observed even after cessation of treatment, most pronouncedly in the SC61 model where no tumor reemergence was seen up to 30 days post treatment in the combination group (Fig. 4E–G). In contrast, xenograft and PDX models with low *BCL2* expression either did not benefit from the combination therapy (Supplementary Fig. 4C,D) or did not exhibit sustained tumor inhibition upon treatment cessation (Supplementary Fig. 4E). Next, to confirm target engagement *in vivo* as well as to investigate the effect on the apoptotic pathway, tumor samples from SC61 PDX models were analyzed 72h post treatment start. As expected, a reduction of phospho Histone H3 (pHH3) levels, indicative of effective AURKB inhibition, was observed in tumors treated with AZD2811NP and the combination therapy. Consistent with the *in vitro* data, AZD2811NP monotherapy induced apoptosis, indicated by increased PARP1 cleavage, which was further increased in the tumors treated with AZD2811NP and venetoclax combination (Fig. 4H).

Next, we also evaluated the optimal dosing and scheduling of an AZD2811NP and venetoclax combination to minimize potential toxicities while achieving sustained tumor inhibition. In the H211 xenograft model, venetoclax was administered on a 7, 5, 3, 2 or 1 day per week schedule in combination with AZD2811NP dosed once weekly (Figure 5A). Of note, the nanoparticle formulation provides slow release of AZD2811 and sustained drug exposure[27]. A continuous daily dosing of venetcolax (7 days per week) in combination with AZD2811NP induced tumor regression of 87% (Figure 5A). In comparison, a reduced venetoclax dosing frequency of 5 days per week or only 3 days per week was still sufficient to achieve significant tumor regression (65% and 62% respectively) (Figure 5A–B). Reducing concurrent venetoclax dosing further to only 1 or 2 days per week did not increase the efficacy of the combination beyond that of AZD2811 monotherapy (Figure 5A). Interestingly, if the sequence of dosing was staggered and venetoclax was administered two days after AZD2811 NP, then only two doses of venetoclax were sufficient to achieve the same level of tumor regression as that obtained with 5 days per week concurrent dosing of venetoclax with AZD2811NP, suggesting that the dose and schedule of this combination could be optimized to increase the therapeutic index (Fig. 5A–B). To further test this hypothesis, three SCLC PDX models were treated with AZD2811NP and venetoclax on a staggered three days a week dosing schedule (Fig. 5C). In addition, we also tested the combination of AZD2811NP with AZD0466 (a drug-dendrimer conjugate of the BCL2/xL dual inhibitor AZD4320)[35]. Administration of both venetoclax and AZD0466 was done one day after AZD2811NP dosing, as indicated (Fig. 5C). The combination of AZD2811NP with either venetoclax or AZD0466 induced similar tumor growth inhibition in all tested models and these values were comparable to those obtained with continuous dosing of venetoclax (Fig. 5C). Altogether, these data demonstrate that venetoclax dosing frequency or schedule allow for modifications, which could reduce potential clinical toxicities but without compromising the efficacy of the combination.

Discussion

RB1 deficiency has been shown to disrupt microtubule dynamics and exacerbate mitotic abnormalities, resulting in an increased sensitivity to AURKB inhibition[22,36]. Therefore, AURKB has emerged as an attractive therapeutic target in SCLC which exhibits a near universal loss of function of *RB1* as well as *TP53*[3]. The results of our study however show that despite near ubiquitous RB1 inactivation, additional factors influence response to AURKB inhibitors in SCLC. Using unbiased proteomic approaches, we identified BCL2 as a key driver of intrinsic resistance to AURKB inhibitors in SCLC cells.

The anti-apoptotic BCL2 family proteins, including BCL2 and BCL-xL, have been shown to be critical for survival from mitotic catastrophe and apoptotic cell death[32]. Polyploidization, such as induced by AURKB inhibitors, has also been shown to result in MCL1 reduction and to shift the anti-apoptotic burden onto BCL-xL in colon carcinoma cells[32]. Accordingly, synergistic interactions between AURKB inhibitors and BCL-xL inhibition have been demonstrated in colon carcinoma and other cancers[32,34]. Polyploidy induced by AURKB inhibition also triggers cell death through lethal autophagy, which is regulated by both BCL2 and BCL-xL[24,37]. In SCLC, BCL2 overexpression as well as BCL-xL amplification have been reported[4,29], and BCL-xL levels are also modestly correlated with BCL2 expression. However, our results show that BCL2, rather than BCL-xL, plays a predominant role in protecting against AURKB-induced cell death in SCLC.

cMYC has previously been identified as a biomarker of sensitivity to AURK inhibitors in SCLC[6,10,15,16,18]. A retrospective study showed improved clinical outcomes in a subset of cMYC-high relapsed SCLC patients receiving the AURKA inhibitor alisertib and paclitaxel, as compared to chemotherapy alone[19]. cMYC has also been shown to epigenetically represses *BCL2*, shifting the apoptotic dependency to MCL1 in SCLC[10]. Given that AURKB inhibition also reduces MCL-1 stability[32], we found several cMYC-overexpressing SCLC cells were sensitive to AURKB inhibitors. Mechanistically, a synthetic lethal interaction between cMYC and AUKRB inhibition, mediated by apoptosis as well as lethal autophagy, has been reported previously[24]. Consistent with this, we found that cMYC-high SCLC cell lines, with low BCL2 levels, that were sensitive to the AURKB inhibitor AZD2811 underwent robust apoptotic cell death. cMYC overexpression is also frequently seen in the NEUROD1-driven SCLC cell lines, which were previously reported to be sensitive to AZD2811[17]. However, amplification of MYC family genes including *MYC* is observed in only 20% of SCLC patients[3]. In contrast, there is high prevalence of BCL2 expression in SCLC[28,29]. We show here that high BCL2 expression strongly predicts resistance to AURKA and AURKB inhibitors. Our analyses also revealed an appreciable number of SCLC cell lines and tumors with concurrent overexpression of both cMYC and BCL2. Cooperative interaction between the two, wherein high BCL2 expression mitigates the mitotic stress and apoptosis induced due to cMYC-overexpression, has been described previously[38]. Importantly, we found that a majority of these SCLC cell lines overexpressing both cMYC and BCL2 were resistant to AZD2811, thus suggesting that some of the cMYC-high SCLC could also benefit from the combined inhibition of AURKB and BCL2. Overall, we show that while cMYC-high/BCL2-low status predicted sensitivity, BCL2-high levels were associated with resistance to AURKB inhibition in SCLC, independent of cMYC.

AURKB inhibitors are in clinical trials in SCLC, other advanced solid tumors and hematologic malignancies as monotherapy and in combination with other drugs (NCT03216343, NCT04830813, NCT01118611, NCT05505825). However, the limited activity in unselected patient populations and dose-limiting toxicity issues have hampered the clinical success of AURKB inhibitors[12]. There is also the added concern that cancer cells surviving AURKB-induced polyploidy could result in increased tumor heterogeneity and therapeutic resistance[39]. BCL2 paralogs have also been explored as potential targets in SCLC[40–42]. A BCL-2/BCL-xL dual inhibitor (navitoclax) showed limited response as monotherapy in refractory metastatic SCLC with dose-dependent thrombocytopenia[43]. On the other hand, the selective BCL2 inhibitor, venetoclax, FDA approved for treatment of relapsed chronic lymphocytic leukemia, is well-tolerated and has minimal dose-limiting toxicities, often seen with BCL-xL inhibitors[44]. Our data demonstrates that sustained SCLC tumor regression can be achieved even with intermittent dosing of AZD2811 and venetoclax, while offsetting potential dose-limiting toxicities. In conclusion, this study provides compelling evidence for the combination of AURKB and BCL2 inhibitors as a useful therapeutic strategy to overcome inherent resistance to AURKB inhibition in SCLC, especially in the BCL2-high patient population. As such, this combination could help in broadening the response to AURKB inhibitors to a larger subset of SCLC.

Supplementary Material

Refer to Web version on PubMed Central for supplementary material.

Acknowledgements

This work was funded by grants from NCI UT Lung SPORE grant CA070907 (L. Byers, J. Wang), and also supported by grants from NIH R01 CA207295 (L. Byers), U01 CA213273 (L. Byers), U01 CA256780 (L. Byers), NIH CCSG P30-CA016672 (L. Byers, J. Wang), R50 CA243698 (A. Stewart) and the Lung cancer moonshot program (L. Byers, J. Wang, C. Gay). The authors also wish to thank the U.T. MD Anderson Flow Cytometry and cellular imaging facility, which is supported in part by NIH through the MD Anderson Cancer Center support grant CA016672, for providing support with FACS analysis. AZD2811 and AZD2811NP was generously provided by AstraZeneca, UK.

References

1. Noone A, et al. SEER cancer statistics review, 1975–2015. Bethesda, MD: National Cancer Institute (2018).
2. Byers LA & Rudin CM Small cell lung cancer: where do we go from here? Cancer 121, 664–672 (2015). [PubMed: 25336398]
3. George J, et al. Comprehensive genomic profiles of small cell lung cancer. Nature 524, 47–53 (2015). [PubMed: 26168399]
4. Kim YH, et al. Combined microarray analysis of small cell lung cancer reveals altered apoptotic balance and distinct expression signatures of MYC family gene amplification. Oncogene 25, 130–138 (2006). [PubMed: 16116477]
5. Peifer M, et al. Integrative genome analyses identify key somatic driver mutations of small-cell lung cancer. Nat Genet 44, 1104–1110 (2012). [PubMed: 22941188]
6. Sos ML, et al. A framework for identification of actionable cancer genome dependencies in small cell lung cancer. Proc Natl Acad Sci U S A 109, 17034–17039 (2012). [PubMed: 23035247]
7. Willems E, et al. The functional diversity of Aurora kinases: a comprehensive review. Cell Div 13, 7 (2018). [PubMed: 30250494]

8. Carmena M, Wheelock M, Funabiki H & Earnshaw WC The chromosomal passenger complex (CPC): from easy rider to the godfather of mitosis. Nat Rev Mol Cell Biol 13, 789–803 (2012). [PubMed: 23175282]

9. Krenn V & Musacchio A The Aurora B Kinase in Chromosome Bi-Orientation and Spindle Checkpoint Signaling. Front Oncol 5, 225 (2015). [PubMed: 26528436]

10. Dammert MA, et al. MYC paralog-dependent apoptotic priming orchestrates a spectrum of vulnerabilities in small cell lung cancer. Nat Commun 10, 3485 (2019). [PubMed: 31375684]

11. Bogen D, et al. Aurora B kinase is a potent and selective target in MYCN-driven neuroblastoma. Oncotarget 6, 35247–35262 (2015). [PubMed: 26497213]

12. Bavetsias V & Linardopoulos S Aurora Kinase Inhibitors: Current Status and Outlook. Front Oncol 5, 278 (2015). [PubMed: 26734566]

13. Goldenson B & Crispino JD The aurora kinases in cell cycle and leukemia. Oncogene 34, 537–545 (2015). [PubMed: 24632603]

14. Keen N & Taylor S Mitotic drivers--inhibitors of the Aurora B Kinase. Cancer Metastasis Rev 28, 185–195 (2009). [PubMed: 19189202]

15. Helfrich BA, et al. Barasertib (AZD1152), a Small Molecule Aurora B Inhibitor, Inhibits the Growth of SCLC Cell Lines In Vitro and In Vivo. Mol Cancer Ther 15, 2314–2322 (2016). [PubMed: 27496133]

16. Mollaoglu G, et al. MYC Drives Progression of Small Cell Lung Cancer to a Variant Neuroendocrine Subtype with Vulnerability to Aurora Kinase Inhibition. Cancer Cell 31, 270–285 (2017). [PubMed: 28089889]

17. Gay CM, et al. Patterns of transcription factor programs and immune pathway activation define four major subtypes of SCLC with distinct therapeutic vulnerabilities. Cancer Cell 39, 346–360 e347 (2021). [PubMed: 33482121]

18. Cardnell RJ, et al. Protein expression of TTF1 and cMYC define distinct molecular subgroups of small cell lung cancer with unique vulnerabilities to aurora kinase inhibition, DLL3 targeting, and other targeted therapies. Oncotarget 8, 73419–73432 (2017). [PubMed: 29088717]

19. Owonikoko TK, et al. Randomized Phase II Study of Paclitaxel plus Alisertib versus Paclitaxel plus Placebo as Second-Line Therapy for SCLC: Primary and Correlative Biomarker Analyses. J Thorac Oncol 15, 274–287 (2020). [PubMed: 31655296]

20. Wilkinson RW, et al. AZD1152, a selective inhibitor of Aurora B kinase, inhibits human tumor xenograft growth by inducing apoptosis. Clin Cancer Res 13, 3682–3688 (2007). [PubMed: 17575233]

21. Johnson ML, et al. Safety, tolerability, and pharmacokinetics of Aurora kinase B inhibitor AZD2811: a phase 1 dose-finding study in patients with advanced solid tumours. Br J Cancer (2023).

22. Oser MG, et al. Cells Lacking the RB1 Tumor Suppressor Gene Are Hyperdependent on Aurora B Kinase for Survival. Cancer Discov 9, 230–247 (2019). [PubMed: 30373918]

23. Cardnell RJ, et al. Activation of the PI3K/mTOR Pathway following PARP Inhibition in Small Cell Lung Cancer. PLoS One 11, e0152584 (2016). [PubMed: 27055253]

24. Yang D, et al. Therapeutic potential of a synthetic lethal interaction between the MYC proto-oncogene and inhibition of aurora-B kinase. Proc Natl Acad Sci U S A 107, 13836–13841 (2010). [PubMed: 20643922]

25. Hook KE, et al. An integrated genomic approach to identify predictive biomarkers of response to the aurora kinase inhibitor PF-03814735. Mol Cancer Ther 11, 710–719 (2012). [PubMed: 22222631]

26. Stewart CA, et al. Single-cell analyses reveal increased intratumoral heterogeneity after the onset of therapy resistance in small-cell lung cancer. Nature Cancer, 1–14 (2020). [PubMed: 35121840]

27. Ashton S, et al. Aurora kinase inhibitor nanoparticles target tumors with favorable therapeutic index in vivo. Sci Transl Med 8, 325ra317 (2016).

28. Ben-Ezra JM, Kornstein MJ, Grimes MM & Krystal G Small cell carcinomas of the lung express the Bcl-2 protein. Am J Pathol 145, 1036–1040 (1994). [PubMed: 7977636]

29. Jiang SX, Sato Y, Kuwao S & Kameya T Expression of bcl-2 oncogene protein is prevalent in small cell lung carcinomas. J Pathol 177, 135–138 (1995). [PubMed: 7490679]

30. Keen N & Taylor S Aurora-kinase inhibitors as anticancer agents. Nat Rev Cancer 4, 927–936 (2004). [PubMed: 15573114]
31. Ditchfield C, et al. Aurora B couples chromosome alignment with anaphase by targeting BubR1, Mad2, and Cenp-E to kinetochores. J Cell Biol 161, 267–280 (2003). [PubMed: 12719470]
32. Shah OJ, et al. Bcl-XL represents a druggable molecular vulnerability during aurora B inhibitor-mediated polyploidization. Proc Natl Acad Sci U S A 107, 12634–12639 (2010). [PubMed: 20616035]
33. Yang J, et al. AZD1152, a novel and selective aurora B kinase inhibitor, induces growth arrest, apoptosis, and sensitization for tubulin depolymerizing agent or topoisomerase II inhibitor in human acute leukemia cells in vitro and in vivo. Blood 110, 2034–2040 (2007). [PubMed: 17495131]
34. Murai S, Matuszkiewicz J, Okuzono Y, Miya H & R, D.E.J. Aurora B Inhibitor TAK-901 Synergizes with BCL-xL Inhibition by Inducing Active BAX in Cancer Cells. Anticancer Res 37, 437–444 (2017). [PubMed: 28179288]
35. Patterson CM, et al. Design and optimisation of dendrimer-conjugated Bcl-2/x(L) inhibitor, AZD0466, with improved therapeutic index for cancer therapy. Commun Biol 4, 112 (2021). [PubMed: 33495510]
36. Lyu J, et al. Synthetic lethality of RB1 and aurora A is driven by stathmin-mediated disruption of microtubule dynamics. Nat Commun 11, 5105 (2020). [PubMed: 33037191]
37. Zhang J, et al. The anti-apoptotic proteins Bcl-2 and Bcl-xL suppress Beclin 1/Atg6-mediated lethal autophagy in polyploid cells. Exp Cell Res 394, 112112 (2020). [PubMed: 32473226]
38. Fanidi A, Harrington EA & Evan GI Cooperative interaction between c-myc and bcl-2 proto-oncogenes. Nature 359, 554–556 (1992). [PubMed: 1406976]
39. Tagal V & Roth MG Loss of Aurora Kinase Signaling Allows Lung Cancer Cells to Adopt Endoreplication and Form Polyploid Giant Cancer Cells That Resist Antimitotic Drugs. Cancer Res 81, 400–413 (2021). [PubMed: 33172929]
40. Lochmann TL, et al. Venetoclax Is Effective in Small-Cell Lung Cancers with High BCL-2 Expression. Clin Cancer Res 24, 360–369 (2018). [PubMed: 29118061]
41. Shoemaker AR, et al. Activity of the Bcl-2 family inhibitor ABT-263 in a panel of small cell lung cancer xenograft models. Clin Cancer Res 14, 3268–3277 (2008). [PubMed: 18519752]
42. Hann CL, et al. Therapeutic efficacy of ABT-737, a selective inhibitor of BCL-2, in small cell lung cancer. Cancer Res 68, 2321–2328 (2008). [PubMed: 18381439]
43. Rudin CM, et al. Phase II study of single-agent navitoclax (ABT-263) and biomarker correlates in patients with relapsed small cell lung cancer. Clin Cancer Res 18, 3163–3169 (2012). [PubMed: 22496272]
44. Davids MS, et al. Comprehensive Safety Analysis of Venetoclax Monotherapy for Patients with Relapsed/Refractory Chronic Lymphocytic Leukemia. Clin Cancer Res 24, 4371–4379 (2018). [PubMed: 29895707]
45. Ramkumar K, et al. AXL Inhibition Induces DNA Damage and Replication Stress in Non-Small Cell Lung Cancer Cells and Promotes Sensitivity to ATR Inhibitors. Mol Cancer Res 19, 485–497 (2021). [PubMed: 33172976]
46. Benjamini Y & Hochberg Y Controlling the false discovery rate: a practical and powerful approach to multiple testing. J. R. Stat. Soc. B 57, 289–300 (1995).

Translational relevance

AURKB targeting is a promising therapeutic strategy in SCLC given the mitotic abnormalities induced by ubiquitous RB1 deficiency. However, preclinical responses and clinical testing of AURKB inhibitors have been limited to only a small subset of SCLC. Using cell lines and patient-derived xenograft models, we show here that BCL2, frequently overexpressed in SCLC, is a strong predictor of resistance to AURKB inhibitors. Response to AURKB inhibition could be significantly enhanced by combining with a BCL2 inhibitor, particularly in SCLC with high BCL2 expression. This study also demonstrates efficacy and tolerability with intermittent dosing schedules of the two drugs, and provides compelling evidence for the rational combination of AURKB and BCL2 inhibitors for SCLC patients.

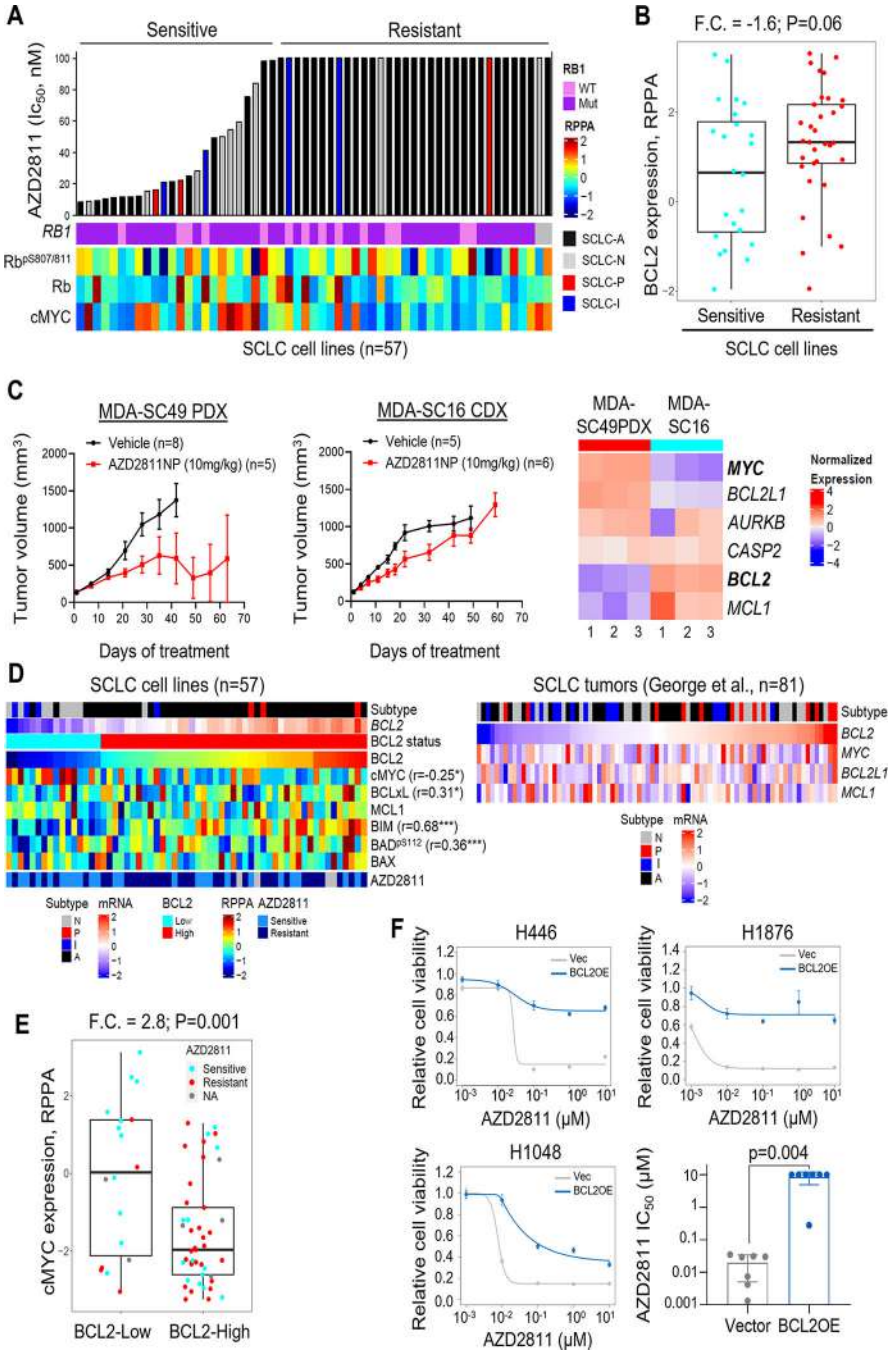

Figure 1. BCL2 is a biomarker of resistance to AURKB inhibition in SCLC.

(A) *In vitro* growth inhibitory activity (IC_{50}, nM) of the selective AURKB inhibitor AZD2811 in a panel of 57 human SCLC cell lines, representing the four distinct SCLC subtypes. Cell lines that did not reach IC_{50} at the highest concentration tested (100nM) were classified as resistant and those with IC_{50} values <100 nM were classified as sensitive. Bars colored by SCLC subtypes. Genomic status of *RB1* and protein expression of phospho and total RB1, and cMYC are annotated in the heatmap below. (B) BCL2 expression, measured by RPPA, between AZD2811-sensitive and -resistant SCLC cell lines. Fold change (F.C.) in

expression between the sensitive and the resistant group, and p-value by t-test are indicated. (C) Athymic nude mice implanted with SC49PDX or SC16 CDX tumors were treated with AZD2811 NP (10 mg/kg, i.v., weekly). Tumor volumes (mean±s.e.m.) are shown. Expression of *MYC*, *AURKB* and *BCL2* family genes in the two models are shown in the heatmap. (D) Expression of BCL2 family members - anti-apoptotic (BCL2, BCL-xL) and MYC in human SCLC cell lines and SCLC patient tumors. AZD2811 sensitivity of SCLC cell lines is annotated. (E) cMYC expression in BCL2-low and BCL2-high SCLC cell lines, classified based on bimodal index cutoff. Dots are colored by AZD2811 sensitivity. Fold change (F.C.) in expression between the BCL2-low and the BCL2-high groups, and p-value by t-test are indicated. (F) Relative viabilities of SCLC cell lines (H446, H1876, H1048), stably overexpressing BCL2, treated with AZD2811 at different concentrations as indicated for 96 h, compared to the vector control cells. Data are mean±s.d. Bar plot shows a comparison of AZD2811 IC_{50} values in different isogenic SCLC cell line pairs (n=7) with and without BCL2 overexpression. p-value by paired t-test.

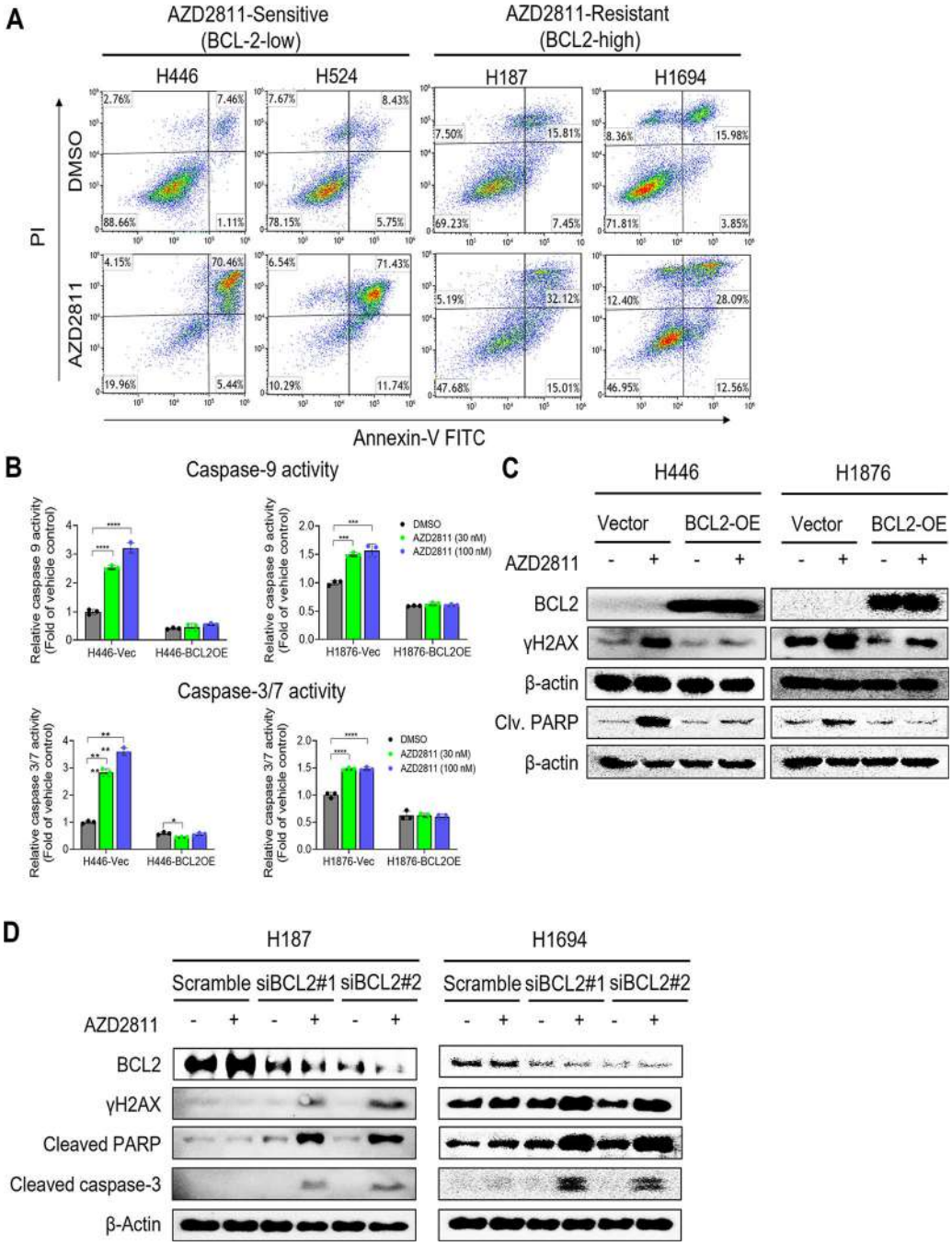

Figure 2. BCL2 overexpression suppresses apoptosis and DNA damage induced by AZD2811, driving resistance.

(A) FACS analysis of Annexin-V and PI staining in representative sensitive and resistant SCLC cell lines, following treatment with AZD2811 (30 nM) for 72 h. (B) Caspase-9 and caspase-3/7 activities in BCL2-overexpressing or vector control SCLC cells treated with AZD2811 or DMSO as indicated for 72 h. Mean±s.d. of triplicate measurements is shown. p-values by one-way ANOVA. (C) Expression of BCL2, markers of apoptosis (cleaved PARP) and DNA damage (γH2AX) by western blotting, following treatment with AZD2811 (30 nM) or DMSO for 48 h, in BCL2-overexpressing and vector control SCLC cell lines.

β-actin was used as loading control. (D) Expression of cleaved PARP, cleaved Caspase-3 and γH2AX in BCL2-high SCLC cell lines treated with AZD2811 (30 nM) for 48 h, following BCL2 knockdown.

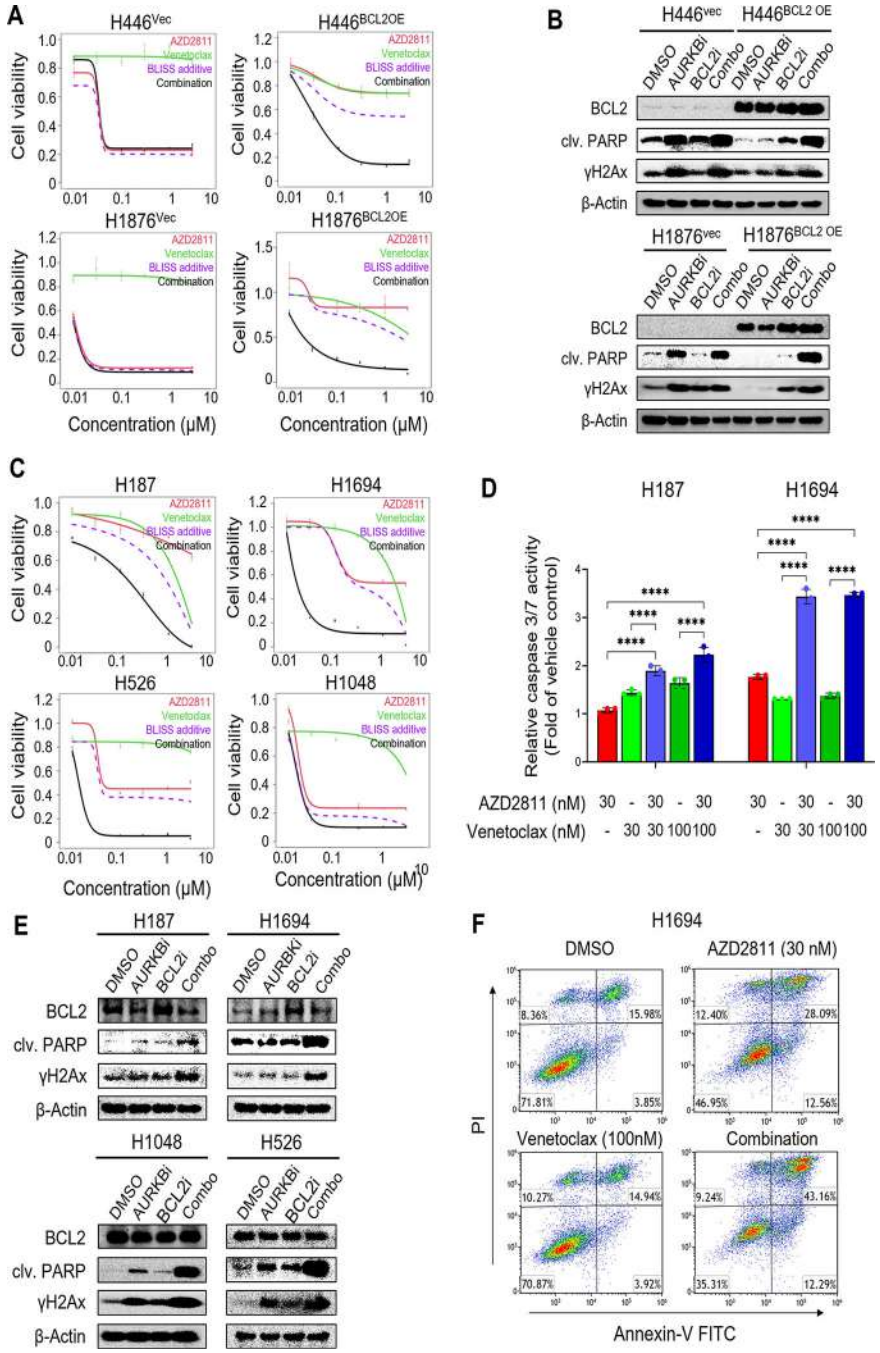

Figure 3. Pharmacological inhibition of BCL2 with venetoclax enhances sensitivity to AZD2811.

(A) Cell viabilities, relative to DMSO treated controls, of isogenic SCLC cell lines stably overexpressing BCL2 or vector control, treated with AZD2811, venetoclax or their combination, as indicated, for 96 h. An additive combinatorial effect, predicted by the BLISS model of synergy is indicated. (B) Expression of BCL2, cleaved PARP and γH2AX following treatment with DMSO, AZD2811 (AURKBi), venetoclax (BCL2i) or their combination for 48 h in the isogenic SCLC cell lines with and without BCL2 overexpression, measured by western blotting. β-actin was used a loading control. (C)

Viabilities of BCL2-high SCLC cell lines treated with AZD2811, venetoclax or their combination. Mean±s.e.m. of triplicate wells are plotted. A predicted additive effect by the BLISS model is indicated. (D) Caspase-3/7 activity, relative to DMSO control, in BCL2-high SCLC cells treated with AZD2811, venetoclax or their combination, as indicated, for 72 h. p values by one-way ANOVA are indicated. (E) PARP cleavage and γH2AX accumulation in AZD2811-resistant SCLC cells (H187, H1694) treated AZD2811 and venetoclax combination for 48 h, detected by western blotting. β-actin was used a loading control. (F) FACS analysis of PI and Annexin-V staining in BCL2-high SCLC cells (H1694) treated with AZD2811, venetoclax or their combination for 72 h.

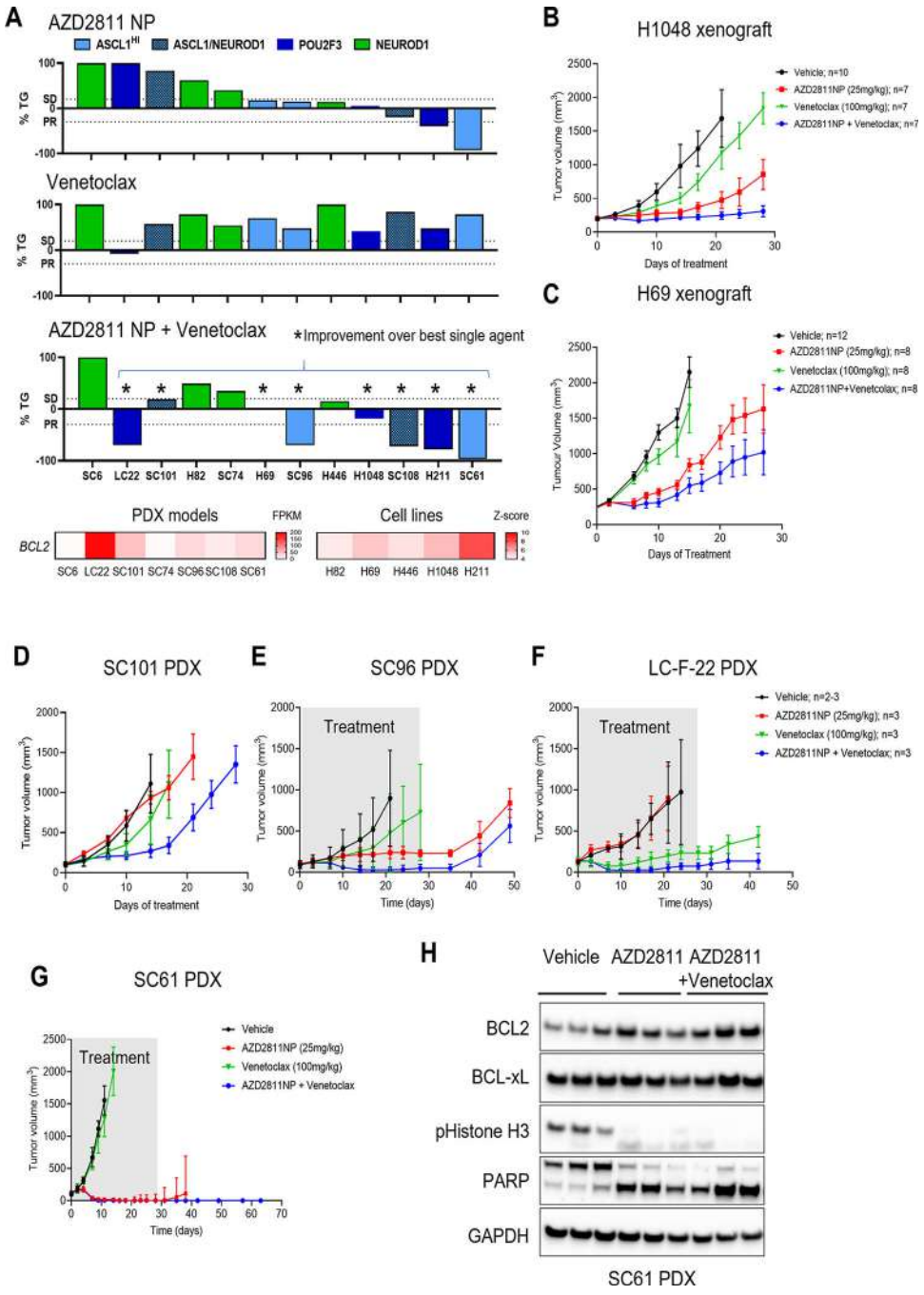

Figure 4. Combination of AZD2811NP with venetoclax results in sustained tumor regression in SCLC xenograft models with high BCL2 expression.

(A) Median best response (%TG) following treatment with AZD2811, venetoclax or their combination in various *in vivo* SCLC models. * denotes improvement over best single agent activity. Bars are colored by mRNA expression of the SCLC subtype markers *ASCL1*, *NEUROD1* and *POU2F3*. Expression levels of *BCL2* in PDX models (RNAseq FPKM values) and in cell lines used for xenografts (Z scores, CCLE) are indicated below. (B-G) Tumor growth curves of SCLC xenograft and PDX models, H1048 (B), H69 (C), SC101 PDX (D), SC96 PDX (E) LC-F-22 PDX (F) and SC61 PDX (G), treated with vehicle

(0.9% saline), AZD2811NP (25 mg/kg, i.v., by tail vein injection weekly), venetoclax (100 mg/kg, p.o., q.d.) or their combination, as indicated. Geomean ± SEM values are plotted. n represents the number of mice used per arm. For all the PDX models, n=3 mice per arm were used with the exception of LC-F-22 where only 2 mice for vehicle group could be included. Duration of treatment in E-G is highlighted by the grey box. (H). Immunoblot of tumor lysates (n=3) from SC61 PDX model 72h after treatment with vehicle (0.9% saline), AZD2811NP (25 mg/kg, i.v. by tail vein, weekly) monotherapy and combination with venetoclax (100mg/kg).

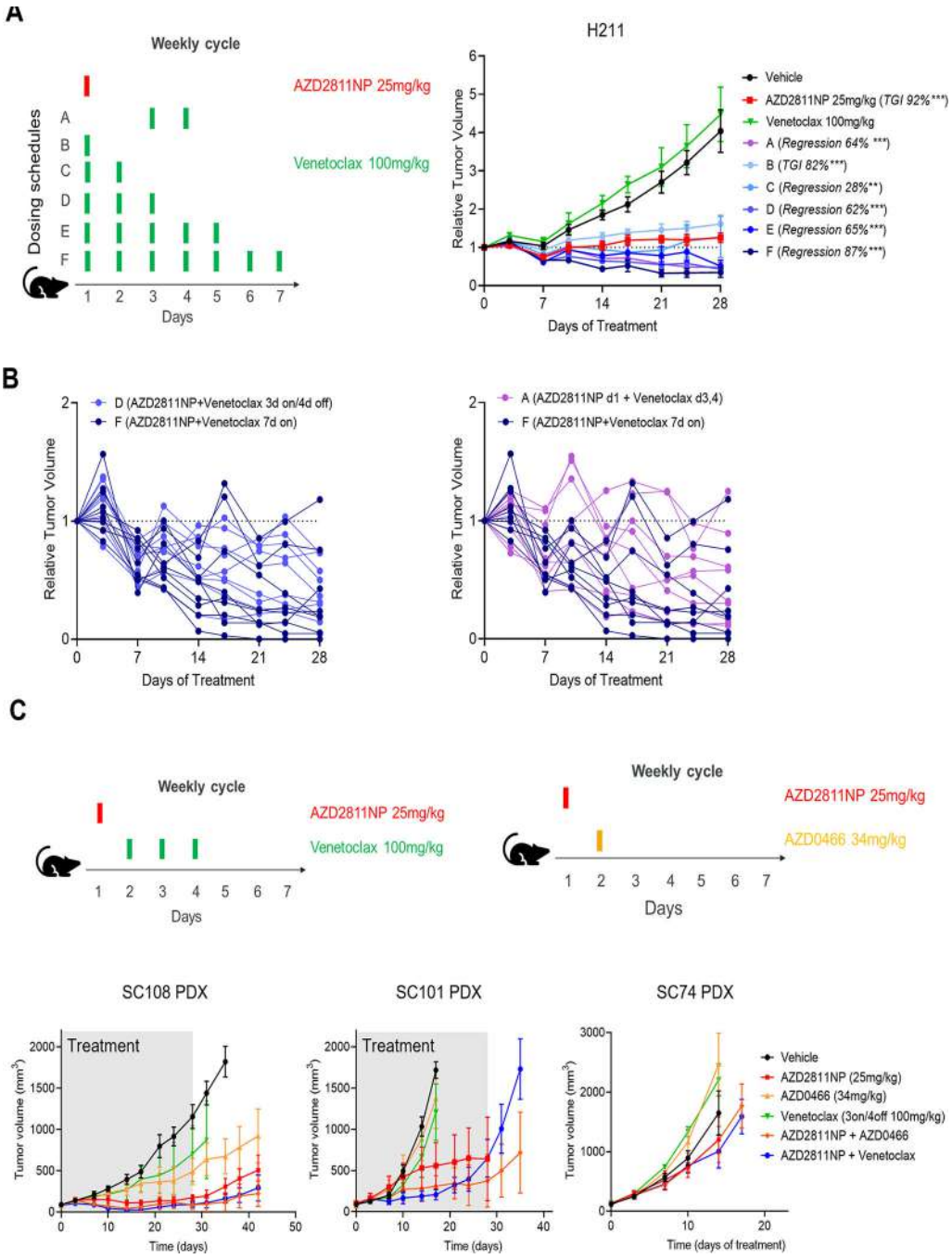

Figure 5. AZD2811 with intermittent dosing of a BCL2 inhibitor retains efficacy *in vivo*.

(A) A schema of dosing schedules used for the treatment of H211 xenograft model (left). Tumor growth volumes for H211 xenograft model following treatment with vehicle, AZD2811 NP (25 mg/kg, i.v. by tail vein, weekly), venetoclax (100 mg/kg, p.o., q.d.) or the combination (right). Percent tumor growth inhibition (TGI) or regression are indicated, and the level of significance was calculated using t-test. n=9 mice were used in each treatment arm. (B) Individual tumor growth volumes for H211 xenograft model following treatment with venetoclax (100 mg/kg, p.o.) in combination with AZD2811NP according to

the different treatment schedules. (C) A schema of dosing schedules used for treatment with AZD2811 in combination with venetoclax or AZD0466 are represented in the top panel. Bottom panel shows tumor growth curves in the PDX models, SC108 PDX, SC101 PDX and SC74 PDX, following treatment with vehicle, AZD2811 NP (25 mg/kg, i.v. by tail vein, weekly), venetoclax (100 mg/kg, p.o.), AZD0466 (34mg/kg i.v. by tail vein, weekly) or the combinations, as indicated. n=3 mice per treatment arm were used.